Drug Design, Development and Therapy

Dovepress
open access to scientific and medical research

Open Access Full Text Article

ORIGINAL RESEARCH

Mechanism of ShuiJingDan in Treating Acute Gouty Arthritis Flares Based on Network Pharmacology and Molecular Docking

Qingsong Liu[1,2,*], Lunyu Li[2,*], Dan Zheng[1], Songlin Jin[2], Xiaotian Guan[2], Zeting Fu[2], Zhigang Xiong[1], Haili Ding[3]

[1]Sichuan Provincial People's Hospital, University of Electronic Science and Technology of China, Chengdu, People's Republic of China; [2]School of Sports Medicine and Health, Chengdu Sport University, Chengdu, People's Republic of China; [3]Insititute of Sports Medicine and Health, Chengdu Sport University, Chengdu, People's Republic of China

*These authors contributed equally to this work

Correspondence: Haili Ding, No. 2, Gymnasium Road, Chengdu, Sichuan, People's Republic of China, Tel +86 13688467479, Email dingdingtang111@163.com

Purpose: This study examined the underlying mechanisms of SJD's anti-inflammatory and analgesic effects on acute GA flares.

Methods: This study used pharmacology network and molecular docking methods. The active ingredients of ShuiJingDan (SJD) were obtained from the Traditional Chinese Medicine Systems Pharmacology Analysis Platform (TCMSP), and the relevant targets of GA were obtained from the Online Mendelian Inheritance in Man (OMIM) database and Therapeutic Target Database (TTD). The core drug group–target–disease Venn diagram was formed by crossing the active ingredients of SJD and the relevant targets. Gene Ontology (GO) analysis was conducted for functional annotation, DAVID was used for Kyoto Encyclopedia of Genes, and Genomes pathway enrichment analysis, and R was used to find the core targets. The accuracy of SJD network pharmacology analysis in GA treatment was verified by molecular docking simulations. Finally, a rat GA model was used to further verify the anti-inflammatory mechanism of SJD in the treatment of GA.

Results: SJD mainly acted on target genes including IL1B, PTGS2, CXCL8, EGF, and JUN, as well as signal pathways including NF-κB, Toll-like receptor (TLR), IL-17, and MAPK. The rat experiments showed that SJD could significantly relieve ankle swelling, reduce the local skin temperature, and increased the paw withdrawal threshold. SJD could also reduce synovial inflammation, reduced the concentrations of interleukin-1β (IL-1β), IL-8, and COX-2 in the synovial fluid, and suppressed the expression of IL1B, CXCL8, and PTGS2 mRNA in the synovial tissue.

Conclusion: SJD has a good anti-inflammatory effect to treat GA attacks, by acting on target genes such as IL-1β, PTGS2, and CXCL8.

Keywords: ShuiJingDan, gouty arthritis, network pharmacology, molecular docking, IL-1β, COX-2

Introduction

Acute gouty arthritis (GA) flares are mainly caused by the reaction of macrophages and neutrophils with monosodium urate (MSU),[1] and are mainly characterized by redness, swelling, heat, and severe pain in the joints. GA is the most common form of arthritis around the world,[2] and a large number of people suffer from gout-related pain every day. Colchicine, non-steroidal anti-inflammatory drugs (NSAIDs), or glucocorticoids are currently used to treat acute flares of GA,[3] but these drugs often cause adverse reactions such as gastrointestinal bleeding, immunosuppression, and liver injury. There is thus an urgent need to find an efficient, safe, and convenient treatment method. ShuiJingDan (SJD) is an internal formulation of the Department of Chinese Medicine of Sichuan Academy of Medical Sciences and Sichuan Provincial People's Hospital. It consists of Rheum palmatum L., Carthamus tinctorius L., Natrii sulfas, Alum, which has been clinically used for nearly 60 years, but the use of three of them (Rheum palmatum L., Carthamus tinctorius L., Natrii sulfas) has been shown to be more effective in the treatment of gouty arthritis after a lot of clinical practice, and so

Received: 25 August 2023
Accepted: 9 November 2023
Published: 24 November 2023

this study focuses on exploring the anti-inflammatory mechanisms of these three herbs in gouty arthritis. According to previous clinical observations, SJD has a good effect on acute inflammatory diseases, such as acute GA flares, cellulitis,[4] acute hematoma,[5] infusion exudation[6] and chemotherapy-induced phlebitis,[7] acute parotitis, and acute hemorrhoids.[8] The treatment of acute GA flares can quickly relieve the symptoms of joint redness, swelling, heat, and pain; shorten the course of disease; reduce the required dosages of NSAIDs and glucocorticoids; and delay disease progression.[9,10] As a natural drug, SJD has the advantages of high curative effects, low cost, and good safety,[9] but there are few studies on its mechanism of action. It was previously found that SJD can reduce interleukin-1β (IL-1β)- and TNF-α-induced inflammatory factors in the synovial fluid of MSU-induced GA rats,[11] but as a compound formulation, SJD has multiple components and multiple targets. Its anti-inflammatory mechanism is still unclear.

With the rapid development of bioinformatics, network pharmacology analysis, which emphasizes the concept of "network-targeting, multi-component therapy", is very consistent with the overall perspective of Chinese medicine (CM),[12,13] and has been proven to be a powerful tool.[13–15] Since network pharmacology provides a systematic understanding of drug action and disease complexity, pharmacological models are beneficial for dissecting the impact of CM on specific diseases.[13] The application of molecular docking has led to the discovery of many key pharmacodynamic components, revealed the pharmacodynamic basis of complex systems, and improved the efficiency and pertinence of the CM screening process.[16,17] However, computation cannot completely replace experiments, and therefore in many cases it must be combined with other methods to validate the results experimentally for the rational design of polypharmacology.[18]

In the present study, we combine network pharmacology, molecular docking simulations, and experimental validation to elucidate the mechanism of action of SJD in the treatment of acute GA flares. Our results indicate that SJD is a new drug candidate for GA treatment.

Material and Methods

Reagents and Materials

SJD Preparation and Topical Application

SJD was provided by the Department of Traditional Chinese Medicine of Sichuan Provincial People's Hospital. It was made by crushing Rheum palmatumnn L., Carthamus tinctorius L., and Natrii sulfas, and mixing them at a 5:8:1 (w/w/w) ratio. After dissolving the medicine in pure water at a ratio of 1:5 (w/v), the solution was boiled for 1 min, filtered, and absorbed into cotton with a thickness of 1.0–1.5 cm. Next, the liquid was squeezed out and the cotton was applied wet onto the affected joint, covered with polyethylene film, fixed with a bandage, and changed once a day.[11]

Animals

Sprague-Dawley rats were purchased from Chengdu Dashuo Biological Co., Ltd. (Chengdu, Sichuan Province, China) and bred under SPF conditions, with 12-hour day-night cycle light and free access to food and water. The experiment was approved by the Ethics Committee of Chengdu Sport University (2021-43). All procedures were in accordance with the guidelines issued by the China Animal Care Committee.

Equipment and Reagents

MSU was purchased from Sigma-Aldrich (St. Louis, MO, USA, batch number U2875). The electronic thermometer and pain threshold meter were provided by the Institute of Chengdu Sports University. IL-1β and cyclooxygenase 2 (COX-2) ELISA kits were purchased from Elabscience Biotechnology Co., Ltd. (Wuhan, Hubei Province, China, batch number BNDGW4WZ4F, D89SKIVT8A) and the IL-8 ELISA kit was purchased from Jingmei Biotechnology Co., Ltd. (Yancheng, Jiangsu Province, China, batch number 202107). RNA TRIzol reagent was purchased from Hefei Bomei Biotechnology Co., Ltd. (Hefei, Anhui Province, China, batch number BM1144); isopropanol was purchased from Shanghai Sangon Bioengineering Technology Service Co., Ltd. (Shanghai, China, batch number B422BA0020); and the PrimeScript RT reagent Kit and TB Green TM Premix Ex Taq^{TM} II (Tli RNaseH Plus) were purchased from Baori Doctor Biotechnology CoLtd. (Beijing, China, batch numbers RR047A and RR820A).

Network Pharmacology Analysis and Molecular Docking of SJD

Acquisition and Screening of Active Ingredients and Targets for SJD

Candidate chemical components and corresponding protein targets were searched for in the Traditional Chinese Medicine Systems Pharmacology Analysis Platform (TCMSP) database using the Chinese pinyin of palmatumnn L. and Carthamus tinctorius L. as query criteria. With reference to Zhu et al's method of screening effective components of external drugs by using network pharmacology,[19] components with drug-like properties (DL) > 0.18 were considered as possibly having medicinal properties for the human body. The components and corresponding targets obtained from the TCMSP database were screened for activity and pharmacological action on the basis of DL > 0.18. Natrii sulfas ($Na_2SO_4 \cdot 10H_2O$) was searched in the Bioinformatics Analysis Tool for Molecular mechANism of Traditional Chinese Medicine (BATMAN-TCM) database. All drug targets were combined and sorted, duplicate drug targets were eliminated, and a "medicinal materials–chemical composition–drug" target network was established.

Retrieval and Acquisition of Disease Target

The disease target genes related to gout were obtained using the PharmGKB, OMIM, GeneCards, and TTD databases using "gout" as the keyword and limiting the search conditions to "gene" and "Homo sapiens". All target genes were combined and duplicate target genes were eliminated.

Venn Analysis of Potential Targets for the Treatment of GA

The total drug targets and total disease targets were imported into the online mapping platform BioVenn, and the intersection of drug targets and disease targets was obtained, which are the potential targets of SJD for the treatment of GA.

Establishment of Protein–Protein Interaction Networks

The intersection targets obtained by Venn analysis were imported into the STRING database. The species was defined as human, the information on protein–protein interactions (PPIs) was obtained, and the information obtained was imported into Cytoscape to generate a PPI network. The topology of the network was analyzed using the Cytoscape 3.8.0 plug-in cytoNCA, including the degree of centrality (DC), medium centrality (BC), eigenvector centrality (EC), and closeness centrality (CC).

GO Functional Enrichment and KEGG Pathway Enrichment Analyses

The enrichment analysis included functional annotation and signal pathway analyses, taking the *P*-value of enrichment results as reference value. The data downloaded from the online database of Kyoto Encyclopedia of Genes and Genomes (KEGG) and Gene Ontology (GO), cellular component (CC), biological process (BP), and molecular function (MF) were used in this study. Using default parameters for GO and KEGG analyses, the functional categories and signal pathways were screened. The first 20 functional annotations and signal pathways were selected for analysis. The results are displayed in the form of a bar chart and a bubble chart, respectively. The enrichment data of drug targets in the first 20 signal pathways were analyzed.

Preparation of Data of Small-Molecule Ligands and Protein Receptors

Ligand files for small molecules were extracted using PubChem. Three-dimensional conversion of small-molecule ligand files was performed using Chemoffice software. Protein receptor files for the target genes were obtained by searching the BDP website, and then the water molecules and small-molecule ligands for the protein receptor were removed using Pymol software.

Active Pocket Detection and Molecular Docking

VINA software was used to determine the active pocket (where the target is a protein or enzyme and the active site is the domain [active pocket] in which the protein can bind to small-molecule ligands). In addition, VINA software was used to determine the location of small-molecule ligands and protein receptors and to predict the best binding sites of effective CM components and drug core targets. The ligand file and the protein receptor file were introduced into VINA for molecular docking.

Animal Experiments

Experimental Animals and Grouping

In total, 32 adult male rats were randomly divided into 4 groups: the control group (C), model group (M), natural group (N), and SJD treatment group (SJ).

Modeling of Acute GA Flares

After 1 week of adaptive feeding, rats in groups M, N, and SJ were injected with 0.5 mL of 25 mg/mL MSU solution in the right knee joint cavity, and rats in group C were injected with the same dose of normal saline. The contralateral bulge of the joint puncture point was set as the injection success criterion, and the acute GA model was induced by the above method. Swelling of the ankle joint, increased skin temperature, and restricted joint movement were clearly observed in groups M, N, and SJ after 12 h, which proved that the model was established successfully.[20]

Experimental Intervention Protocol

After successful modeling, the SJ group was treated with topical application of SJD, while the C and N groups were treated with topical application of pure water in the same way, once per day for 6 h, for a total of 3 days.

Sample Collection and Preservation

After anesthesia with sodium pentobarbital (ip, 70 mg/kg body weight) 24 hours after molding in group M and 72 hours after intervention in groups C, N, and SJ, 0.5 mL of saline was injected into the right ankle joint and the joint was moved for 1 minute, the ankle skin was incised, the synovial fluid was aspirated with an empty needle, and the synovial fluid was centrifuged at 3000 rpm for 5 minutes and stored at −80°C.

Joint Swelling Degree, Right Ankle Skin Temperature, and Paw Withdrawal Threshold Measurement

The circumference of the same part of the right ankle joint was measured before and after modeling and before sampling using a non-elastic soft tape. This was repeated three times and the resulting values were averaged. The joint swelling degree was calculated as follows: joint swelling degree = (post-modeling joint circumference − pre-modeling joint circumference)/(pre-modeling joint circumference). The local skin temperature of the right hind ankle joint was measured by an electronic thermometer. The right hind limb ankle joint was stimulated bottom-up with von Frey filament as follows: The rat was placed on a grid platform surrounded by a transparent box, and a 15-gauge filament was used to stimulate the rat ankle from below. The paw was retracted due to pain. At this time, the maximum value generated by the force sensor under the filament was taken as the paw retraction threshold. This was repeated five times and the average value was taken.

H&E Staining of Ankle Synovial Membrane

The synovial tissues of each group were fixed in 10% paraformaldehyde solution, and the synovial tissues were decalcified, paraffin-embedded, sectioned, de-paraffinized, hydrated, and stained with H&E. The histopathology of the synovial tissues was observed under a light microscope.

Detection of Synovial Fluid Cytokines by ELISA

The standard operation procedures according to the instructions of the ELISA kits were followed.

Detection of IL1B, CXCL8, and PTGS2 mRNA in Synovial Tissue by Real-Time Quantitative PCR

The entire gene sequence was searched from the National Center for Biotechnology Information (NCBI) database, and gene-specific primers were designed and screened using Premier primer design software. All primers were designed and synthesized by Shanghai Sangon Bioengineering Technology Service Co., Ltd. and purified by ULTRAPAGE. The primer sequences are shown in Table 1. To measure mRNA levels, 50 mg of synovial tissue was taken and total RNA was extracted using TRIzol. The extracted total RNA was reverse transcribed into cDNA following the kit's instructions, and the cDNA was used for real-time quantitative PCR.

Table 1 Primer Sequence Table

Primer	Sequences (5'-3')	
IL1B	Upstream	AGCTACGAATCTCCGACCAC
	Downstream	CGTTATCCCATGTGTCGAAGAA
CXCL8	Upstream	ACGCTGGCTTCTGACAACACTAGT
	Downstream	CTTCTCTGTCCTGAGACGAGAAGG
PTGS2	Upstream	CACATTTGATTGACAGCCCACCAAC
	Downstream	AGTCATCAGCCACAGGAGGAAGG
β-actin	Upstream	GGGAAATCGTGCGTGACATT
	Downstream	GCGGCAGTGGCCATCTC

Statistical Analysis

Data have been presented as mean values ± standard deviation. One-way analysis of variance (ANOVA) with Tukey multiple comparison test is used for data analysis. $P < 0.05$ was considered statistically significant.

Results

Screening of Active Ingredients

The database of CM was searched, using the screening condition DL > 0.18. A total of 27 active ingredients of Rheum palmatumnnL., Carthamus tinctoriusL., and Natrii sulfas, were selected. Among them, rhein, aloe-emodin, quercetin, luteolin, beta-carotene, etc., have a wide range of pharmacological effects, such as anti-inflammatory and antioxidant effects. The targets in the database of active ingredients of CM were retrieved, the target gene names were obtained from the UniProt database, invalid and duplicate targets were deleted, and 221 targets of active ingredients were obtained. A total of 1591 GA gene targets were obtained by searching and integrating the Gene Card, OMIM, PharmGKB, and TTD databases (Figure 1A)

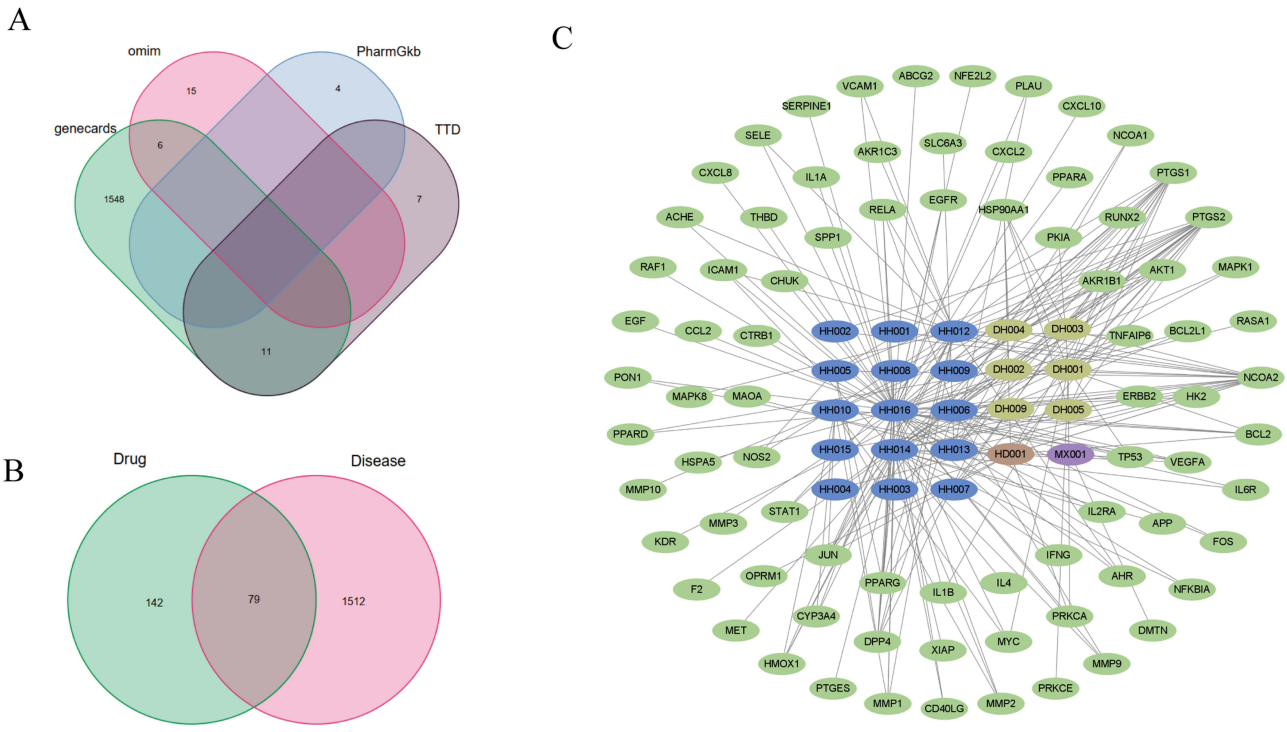

Figure 1 (**A**) The distribution of 1591 disease targets from the GeneCards, OMIM, PharmGKB, and TTD databases. (**B**) Venn diagram of potential targets of SJD for GA treatment. (**C**) The core drug group–target–disease Venn diagram, where green shows the target genes, blue shows the Carthamus tinctorius L. active ingredients, beige shows the active ingredients of Rheum palmatum L., purple shows the active ingredients of mirabilite, and dusky red shows the common active ingredients of Carthamus tinctorius L. and Rheum palmatum L..

and 79 drug–disease common target genes were obtained (Figure 1B). Components without corresponding targets and duplicate targets were excluded, and the resulting 23 drug components (Table 2) and 79 disease-related targets were mapped. Among them, DH represents Rheum palmatum L., HH represents Carthamus tinctorius L., HD represents common ingredients of Carthamus tinctorius L. and Rheum palmatum L., and MX represents Natrii sulfas. The data were imported into Cytoscape to construct the component target network (Figure 1C), where one or more active components can correspond to a target and multiple targets can correspond to the same active component, indicating that the group has a multi-component and multi-target profile for the treatment of GA.

PPI Network and GO and KEGG Enrichment Pathway Analysis

The common targets of SJD for GA treatment were imported into STRING (https://string-db.org/) to construct PPI networks. We obtained the GA-related PPI network. We observed 79 targets that could interact with proteins and 1124 edges representing PPIs, with a mean node degree of 28.5, a mean local clustering coefficient of 0.683, an expected number of edges of 308, and a PPI-enriched *P*-value of < 1.0e−16 (Figure 2A). The results of MF, BP, and CC analysis of 170 core targets showed that the key active components of SJD were highly enriched in 102 GO items, and target proteins were enriched in 158 KEGG pathways. The top 30 GOs were selected to analyze the results with a threshold of $P < 0.05$ to obtain the main pathways of action in the core drug group for the treatment of gout, including the NF-κB, MAPK, Toll-like receptor (TLR), PI3K–Akt, IL-17, TNF, and HIF-1 signaling pathways (Figure 2B and C).

PPI Core Gene Screening

The TSV format data from 32 PPIs were imported into Cytoscape and the PPIs based on DC, BC, CC, EC, NC, and lac parameters were analyzed using cytoNCA. The initial sieve threshold was Degree > 12, Magi Eigenvector > 0.073067062, Lac > 6, Magnetic Closeness > 37.74521856, Magical Closeness > 0.483660131, and Network > 6.75. There were 37 nodes and 163 edges. Then, 37 targets were further screened. Secondary screening thresholds were degree > 27, pr eigenvectors > 0.188253894, prelac > 11.71428571, recall mediator > 168.9082139, pr closeness > 0.587301587, and gradient network > 18.27076629. The second screen yielded 10 nodes with 29 edges, including *JUN, PTGS2, VEGFA, MAPK1, IL1B, CXCL8, EGF, TP53*, and *MAPK8*, suggesting that this could be a potentially important target for the treatment of gout (Figure 3).

Molecular Docking

The core targets of IL1B,[21] CXCL8,[22,23] and PTGS2[24] with the highest correlation with acute gout inflammation were analyzed and extracted, and the core small-molecule ligands (quercetin, emodin, rhein, etc.) were extracted from the

Table 2 Effective Active Ingredients of Drugs

Node	MolId	MolName	Node	MolId	MolName
DH001	MOL000471	Aloe-emodin	HH007	MOL002717	qt_carthamone
DH002	MOL002235	Eupatin	HH008	MOL002721	Quercetagetin
DH003	MOL000096	(-)-catechin	HH009	MOL002757	7,8-dimethyl-1H-pyrimido [5,6-g]quinoxaline-2,4-dione
DH004	MOL002268	Rhein	HH010	MOL002773	Beta-carotene
DH005	MOL002281	Toralactone	HH012	MOL000422	Kaempferol
DH009	MOL002297	Daucosterol_qt	HH013	MOL000449	Stigmasterol
HH001	MOL001771	Poriferast-5-en-3beta-ol	HH014	MOL000006	Luteolin
HH002	MOL002694	4-[(E)-4-(3,5-dimethoxy-4-oxo-1-cyclohexa-2,5-dienylidene) but-2-enylidene]-2,6-dimethoxycyclohexa-2,5-dien-1-one	HH015	MOL000953	CLR
HH003	MOL002695	Lignan	HH016	MOL000098	Quercetin
HH004	MOL002710	Pyrethrin II	HD001	MOL000358	Beta-sitosterol
HH005	MOL002712	6-Hydroxykaempferol	MX001		Na2SO4_10H2O
HH006	MOL002714	Baicalein			

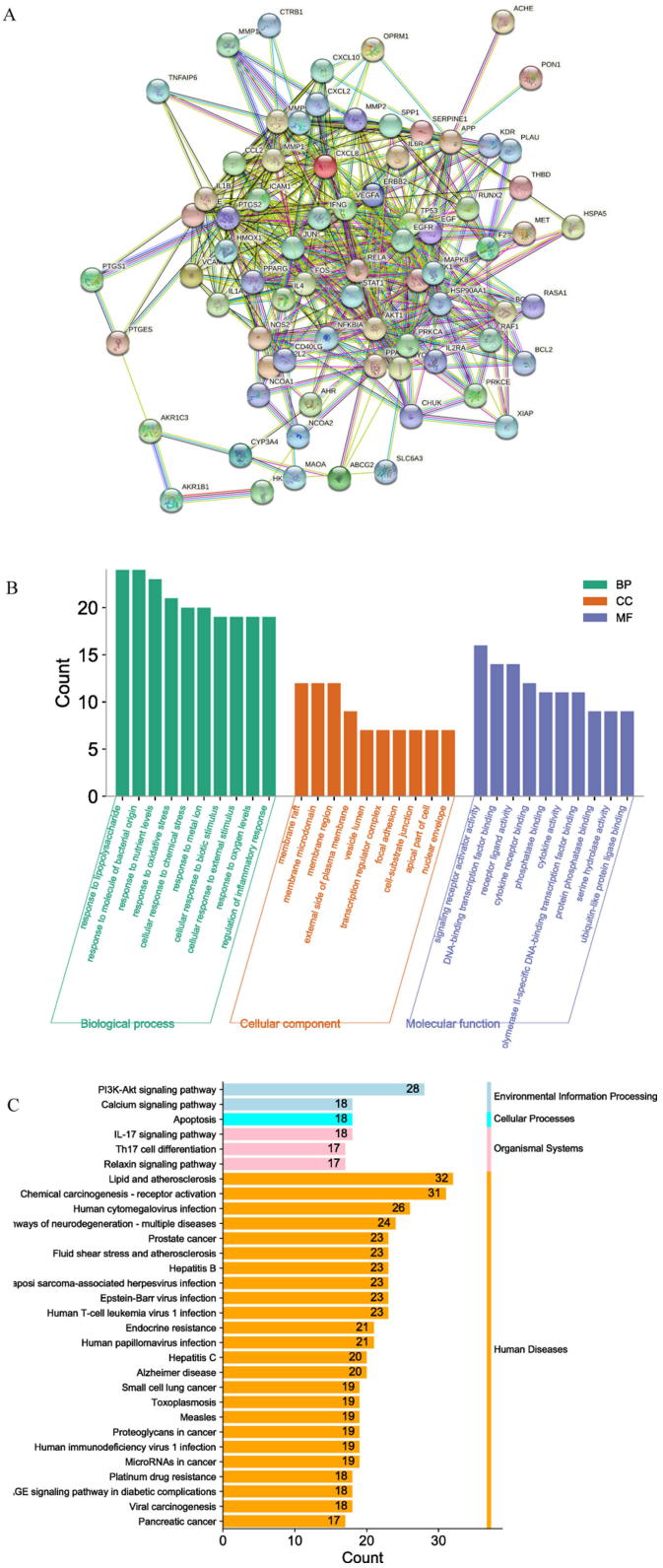

Figure 2 PPI network of disease targets and GO and KEGG enrichment pathway analysis. (**A**) PPI network of disease targets. (**B**) Functional enrichment analysis of GO, the potential targets of SJD for gout treatment. (**C**) 30 KEGG pathways that were highly correlated with SJD treatment for gout.

https://doi.org/10.2147/DDDT.S436360

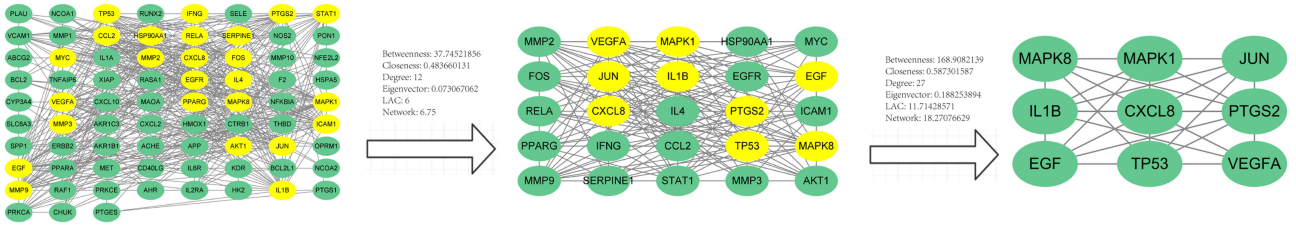

Figure 3 Screening of core targets for SJD in the treatment of gout.

PubChem and PDB databases. The corresponding small-molecule ligands were optimized by Chemo3D software to determine the optimal binding site between the visually effective compound SJD and the gout core target, as well as the molecular docking of core molecular ligands and protein receptors (Figure 4). Yellow in the figure shows hydrogen bond, and molecular binding energy is attached to Table 3.

Animal Experiment Results

Improvement of Acute GA Flare Symptoms by SJD

During the modeling process, one rat in the SJ group suffered lung contusion due to over-tight fixation, so it was excluded from the experiment. Significant swelling, increased local skin temperature, restricted joint movement, and a lower paw withdrawal threshold were observed in the ankle joints of rats in groups M, N, and SJ 12 h after molding, with no statistical difference between them ($P > 0.05$). Group C showed no significant changes in the ankle joint and was statistically different from groups M, N, and SJ ($P < 0.0001$). The rats in group N had a reduced joint circumference, lower local skin temperature, and higher paw withdrawal threshold than rats in group M, with more pronounced changes in group SJ compared to group M (Figure 5).

Effects of SJD on Acute GA Synovial Inflammation

The synovial joint tissue in group C was clear and intact; the lining layer consisted of a single or double layer of synovial cells, with no obvious inflammatory cell infiltration or fibrous tissue hyperplasia. Group M had mild to

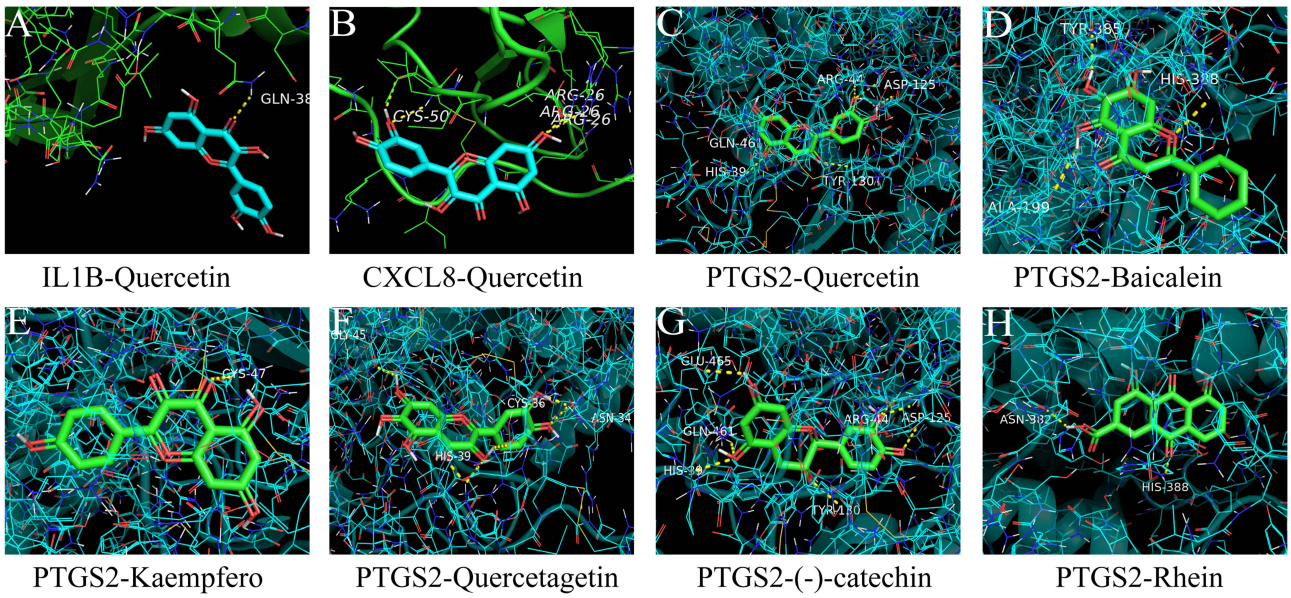

Figure 4 Molecular docking structure of SJD core small-molecule components and key therapeutic targets of gout. (**A**) IL1B-Quercetin; (**B**) CXCL8-Quercetin; (**C**) PTGS2-Quercetin; (**D**) PTGS2-Baicalein; (**E**) PTGS2-Kaempfero; (**F**) PTGS2-Quercetagetin; (**G**) PTGS2-(-)-catechin; (**H**) PTGS2-Rhein.

Table 3 The Binding Energy of Each Molecule to the Protein Exhibit

Core Target	Chemical Composition	Binding Energy/kcal•mol^{-1}
IL1B	Quercetin	−6.4
CXCL8	Quercetin	−6.7
PTGS2	Quercetin	−8.9
PTGS2	Baicalein	−8.9
PTGS2	Kaempfero	−8.7
PTGS2	Quercetagetin	−8.8
PTGS2	(-)-catechin	−8.8
PTGS2	Rhein	−9.0

moderate infiltration of inflammatory cells in the sublayer, mainly lymphocytes with rounded, deeply stained nuclei, neutrophils with rod-shaped or lobulated nuclei, and plasma cells with nuclei on one side of the cell, and localized necrosis with necrotic cell nuclei solidified and disintegrated, cytoplasmic lysis, and more eosinophilic plasma material exuding from the necrotic area. Group N has varying degrees of inflammatory cell infiltration in the sublingual layer, mainly lymphocytes, neutrophils, and plasma cells, with proliferation of fibrous tissue and slight local hemorrhage. Inflammatory cell infiltration was observed in the sublingual layer of the SJ group, dominated by lymphocytes and neutrophils, with an increased number of fibroblasts with long oval or oval nuclei and slight local hemorrhage. The degree of pathological changes was significantly greater in group M compared to group C. Compared to group M, group N had relatively mild pathological changes and group SJ had the least pathological changes (Figure 6).

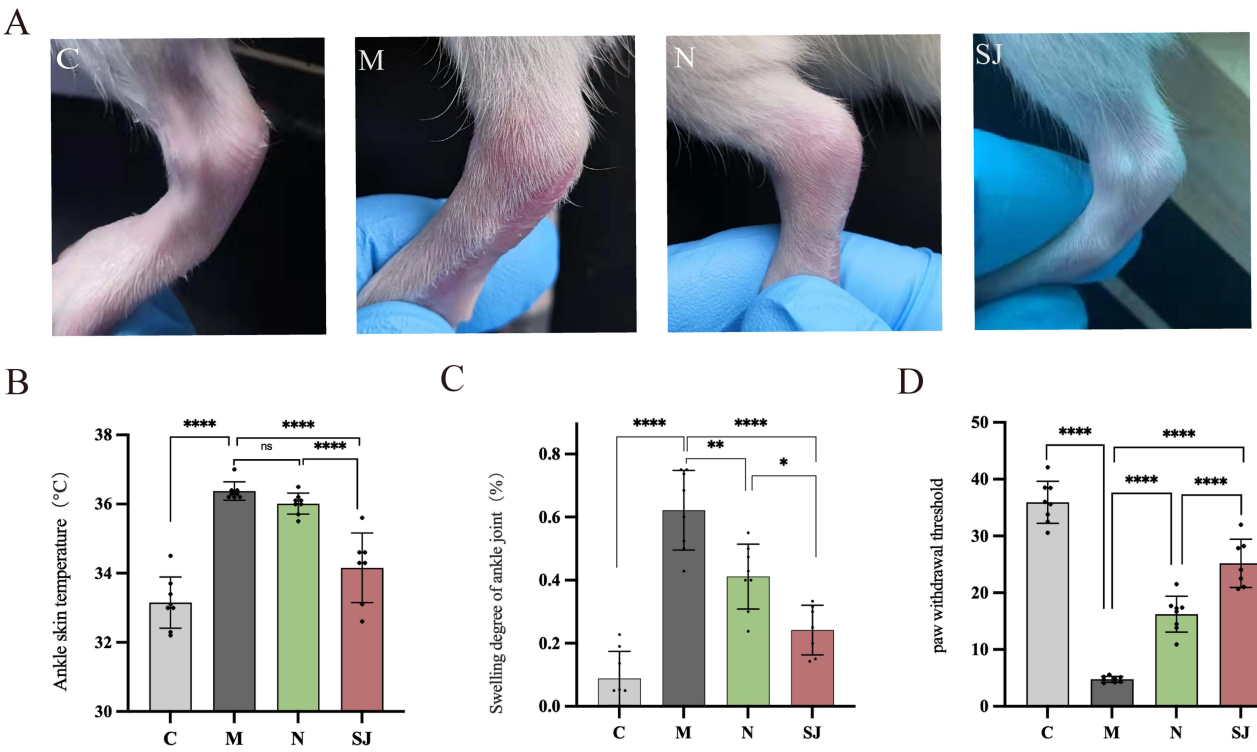

Figure 5 Changes in ankle skin temperature, joint swelling degree, and paw withdrawal threshold. (**A**) The appearance of the ankle joint. GA rats have obvious redness and swelling, and SJD treatment can significantly improve the degree of swelling. (**B**) The skin temperature of the ankle joint. (**C**) The degree of swelling of the ankle joint. (**D**) The von Frey paw withdrawal threshold of the ankle joint. *P < 0.05; **P < 0.01; ****P < 0.0001.
Abbreviation: Ns, not significant.

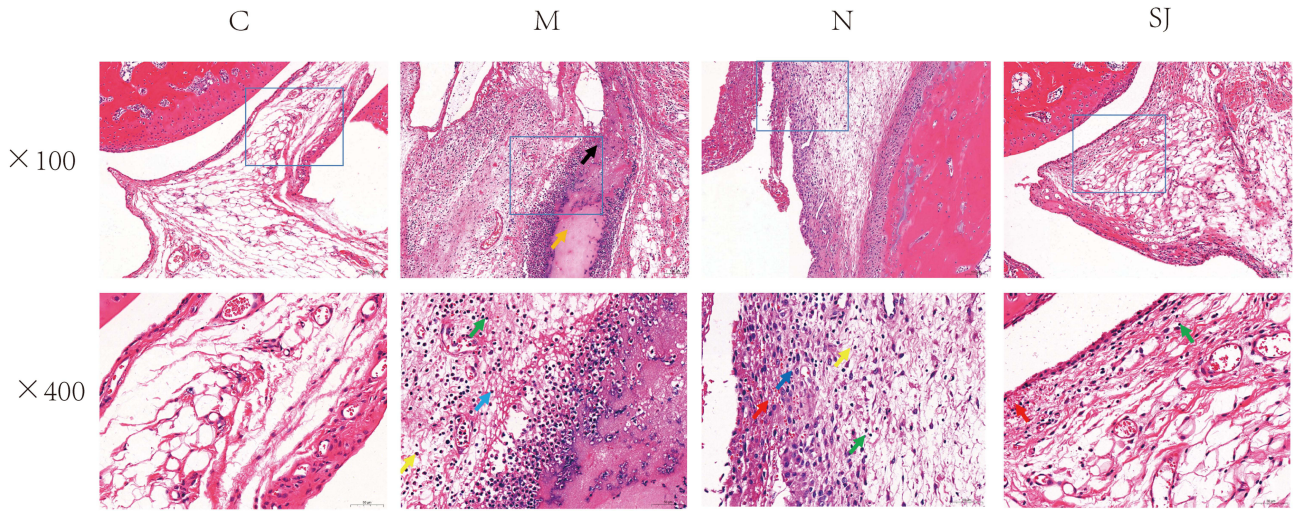

Figure 6 HE staining of ankle joint. Up (×100), down (×400), In the down (×400) of group N,lymphocytes (green↑), neutrophils (yellow↑), fibroblasts (blue↑), and bleeding (red↑).

Effects of SJD on Cytokine and IL1B, CXCL8, and PTGS2 mRNA Expression

MSU crystals can induce the expression of IL-1β, IL-8, and COX-2 in the synovial fluid of rats. Significant differences were observed between groups M and C. MSU crystals can increase the expression of IL1B, CXCL8, and PTGS2 mRNA in synovium. Compared with the non-medicated group N, the external application of SJD significantly reduced the levels of pro-inflammatory factors and IL1B, CXCL8, and PTGS2 mRNA in the synovial fluid of the GA rats (Figure 7).

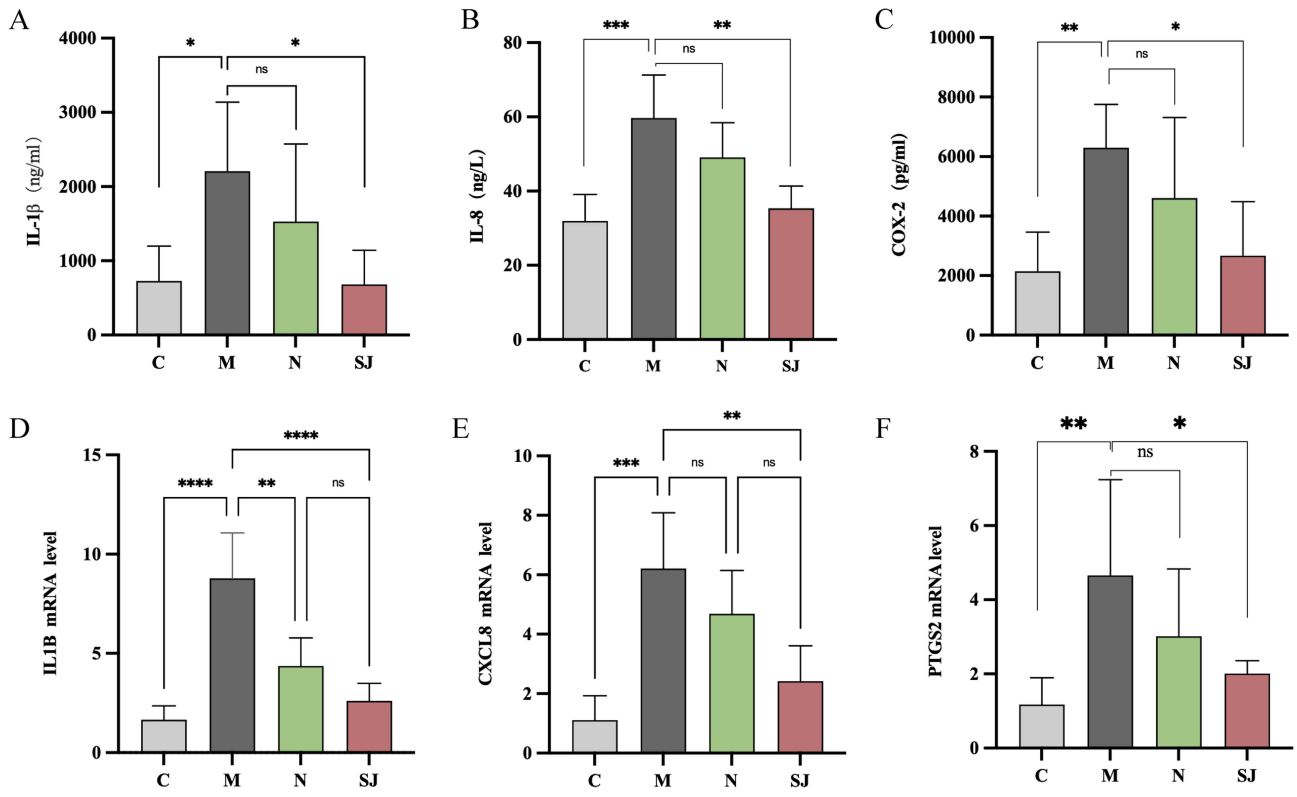

Figure 7 Cytokine concentrations in synovial fluid and IL1B, CXCL8, and PTGS2 mRNA expression in synovium (n_C = 8; n_M = 8; n_N = 8; n_{SJ} = 7). (**A**) IL-1β concentration (ng/mL). (**B**) IL-8 concentration (ng/L). (**C**) COX-2 concentration (ng/L). (**D**) IL1B mRNA expression level. (**E**) CXCL8 mRNA expression level. (**F**) PTGS2 mRNA expression level. *P < 0.05; **P < 0.01; ***P < 0.001; ****P < 0.0001.

Abbreviation: Ns, not significant.

Discussion

SJD is a widely used prescription in Sichuan Provincial People's Hospital, which has good anti-inflammatory effects on acute GA flares. The SJD formula is refined, and the main ingredients are Rheum palmatum L., Carthamus tinctorius L., and Natrii sulfas. In the theory of CM, rhubarb is bitter and cold, and external use can have heat-clearing and detoxifying effects. It can be used to treat acute inflammation. Mirabilite is bitter and cold and can improve local swelling of acute GA flares. Safflower is pungent and warm in nature, which helps to unblock the blood vessels and disperse blood stasis, helping to improve local blood circulation due to acute inflammation.

In this study, 27 active ingredients were screened. Among them, rhubarb acid, aloe rhodopsin, quercetin, lignan, and β-carotene are the main core compounds of SJD for GA treatment. The NLRP3 inflammasome has a prominent role in the pathogenesis of inflammatory arthritis, especially gout.[25] Rhein can inhibit the protease activity of caspase-1 and the pharmacological activity of IL-1, interfering with the NLRP3 complex.[26] β-Carotene can prevent the production of IL-1β and caspase-1, which may have potential as a future therapy for gout.[27] Xanthine oxidase (XO) catalyzes the production of uric acid from hypoxanthine and xanthine in human metabolism. Excessive production of uric acid can lead to hyperuricemia and eventually gout and other diseases. Aloe-emodin derivatives and luteolin can significantly inhibit XO.[28,29] In addition, luteolin can improve the inflammatory response of gout by inhibiting the TLR/MyD88/NF-κB pathway[30] and reducing the levels of IL-1β and TNF-α.[31] Quercetin was found to reversibly inhibit XO activity by 50% and reduce uric acid production, and in in vitro studies, quercetin inhibited COX-I and II activity by 52.8% and 42.3%, respectively.[32]

The results of this study show that the main potential targets of SJD for the treatment of gout are *JUN, PTGS2, VEGFA, MAPK1, IL1B, CXCL8, EGF, TP53*, and *MAPK8*. Among them, COX-2 is a key enzyme that induces the synthesis of prostaglandin E2 (PGE2), and PGE2 is an important factor involved in synovial and periarticular tissue inflammation and glomerular injury lesions.[32,33] In patients with gout, deposited MSU crystals may stimulate the generation of a systemic inflammatory response by upregulating PTGS2 (COX-2 gene) in peripheral mononuclear cells in advanced gout,[34] and selective COX-2 inhibitors are effective and important agents for the treatment of acute attacks of gout[35] to provide rapid relief of joint erythema and pain. Our experiments demonstrated that SJD can rapidly control inflammation by inhibiting PTGS2 gene expression, which seems to explain that SJD has a similar effect to COX-2 selective inhibitors. In gout, IL-1β production is mediated by MSU crystals triggering the inflammasome,[1] and sustained IL-1β secretion induces rapid recruitment of neutrophils to sites of crystal deposition, producing a more severe inflammatory response,[36] as well as inducing the production of matrix-degrading enzymes that break down cartilage and chondrocytes,[37] all of which are key factors in IL-1β-mediated inflammation. CXCL8 (IL-8) levels are increased in the synovial fluid and serum of gout patients independent of their disease activity, but higher CXCL8 levels are associated with cardiovascular disease in gout patients.[38] VEGFA was identified as the locus of hyperuricemia.[39] KEGG pathway enrichment analysis showed that the key pathways involved affected by SJD in gout treatment are the NF-κB, MAPK, and TLR signaling pathways. The NF-κB signaling pathway regulates the production and maturation of IL-1β, which is a key factor causing acute inflammation. The induction of IL-1β release by MSU requires the activation of NF-κB to stimulate the expression of pro-IL-1β.[40] TLRs are transmembrane proteins expressed by cells of the innate immune system; they recognize pathogen-associated molecular patterns and play important roles in immune and inflammatory responses to destroy invaders.[41] MSU interacts with TLR2 and TLR4 of the TLR family, interacting with TLR2 on chondrocytes to induce nitric oxide production, thereby accelerating cartilage degeneration,[42] and interacting with TLR2/TLR4 on macrophages, leading to IL-1β production to induce synovial inflammation.[43]

It has been shown that SJD can quickly relieve the symptoms of acute GA flares, reduce key inflammatory factors, and inhibit inflammation during acute GA flares, and it may have a protective effect on the cardiovascular system of gout patients. SJD is an excellent option as a topical treatment during acute GA flares.

Conclusion

In this study, network pharmacology and molecular docking simulations combined with experimental verification were used to clarify the mechanism of SJD in the treatment of acute GA flares. The network pharmacology and molecular docking simulation results show that SJD mainly acts on target proteins such as IL-1β, IL-8, and COX-2 and regulates

the NF-κB, TLR, IL-17, and MAPK signaling pathways in the treatment of acute GA. In addition, experiments in rats showed that SJD can significantly relieve the symptoms of GA, reduce the important pro-inflammatory factors IL-1β, IL-8, and COX-2 in the synovial fluid, and inhibit the expression of IL1B, CXCL8, and PTGS2 mRNA in the synovium membrane.

Abbreviations

SJD, ShuiJingDan; GA, gouty arthritis; TCMSP, Traditional Chinese Medicine Systems Pharmacology Analysis Platform; OMIM, Online Mendelian Inheritance in Man; TTD, Therapeutic Target Database; GO, Gene Ontology; CC, cellular component; BP, biological process, MF, molecular function; TLR, Toll-like receptor; IL-1β, interleukin-1β; MSU; monosodium urate; NSAIDs, non-steroidal anti-inflammatory drugs; CM, Chinese medicine; COX-2, cyclooxygenase 2; DL, drug-like properties; KEGG, Kyoto Encyclopedia of Genes and Genomes; XO, Xanthine oxidase; PGE2, prostaglandin E2.

Acknowledgments

The work was financially supported by National Natural Science Foundation of China (NSFC) (grant numbers 81904318); the Sichuan Provincial Key Laboratory of Sports Medicine and the State Sports General Administration Key Laboratory (No.2022-A010), and the Sichuan Provincial Administration of Traditional Chinese Medicine Funding Project (Grant No. 2021MS078).

Disclosure

The institution and department of the first author of this article are prescription users of SJD, but like all authors, there is no competing financial interests personal relationships, which does not affect the research results and article reporting.

References

1. So AK, Martinon F. Inflammation in gout: mechanisms and therapeutic targets. *Nat Rev Rheumatol*. 2017;13(11):639–647. doi:10.1038/nrrheum.2017.155
2. Dehlin M, Jacobsson L, Roddy E. Global epidemiology of gout: prevalence, incidence, treatment patterns and risk factors. *Nat Rev Rheumatol*. 2020;16(7):380–390. doi:10.1038/s41584-020-0441-1
3. FitzGerald JD, Dalbeth N, Mikuls T, et al. 2020 American College of Rheumatology guideline for the management of gout. *Arthritis Rheumatol*. 2020;72(6):879–895. doi:10.1002/art.41247
4. Feng J, Deng F, Duan, H. Observation on the efficacy of external application of ShuiJingDan in the treatment of acute honeycomb tissue inflammation. *J Clin Med Pract Hosp*. 2016;13(04):109–111.
5. Liang T, Chen Y. ShuiJingDan external application treatment of radial artery coronary intervention after upper limb hematoma curative effect observation. *Sichuan Med*. 2013;34(09):1316–1317.
6. Xue L, Li H, Zhang, C. Chinese medicine ShuiJingDan external treatment of venous transfusion extravasation curative effect observation. *Pract Hosp Clin J*. 2009;6(01):59–60.
7. P X. ShuiJingDan combined with TDP irradiation treatment of chemotherapeutic phlebitis curative effect observation. *Sichuan Med*. 2012;33(03):559–561.
8. Liu F, CHen X. ShuiJingDan fumigation treatment of hemorrhoids 120 cases. *Mod J Integr Trad Chin Western Med*. 2003;3:275.
9. Duan H, Mu F. Shuijingdan treatment of acute gouty arthritis 135 cases of clinical observation. *Sichuan Med*. 2008;5(10):1347–1348.
10. Xiong Y. Clinical observation of external application of Shuijingdan combined with diet nursing in the treatment of acute gouty arthritis. *Western Med*. 2001;23(10):1992–1994.
11. Wang H. Study on anti-inflammatory mechanism of external application of Shuijingdan on MSU-induced acute gouty arthritis rat model. Chengdu University of Traditional Chinese Medicine. 2020.
12. Jiao X, Jin X, Ma Y, et al. A comprehensive application: molecular docking and network pharmacology for the prediction of bioactive constituents and elucidation of mechanisms of action in component-based Chinese medicine. *Comput Biol Chem*. 2021:90. doi:10.1016/j.compbiolchem.2020.107402
13. Cao H, Li S, Xie R, et al. Exploring the mechanism of Dangguiliuhuang decoction against hepatic fibrosis by network pharmacology and experimental validation. *Front Pharmacol*. 2018;9(MAR). doi:10.3389/fphar.2018.00187
14. Guo Q, Zheng K, Fan D, et al. Wu-Tou decoction in rheumatoid arthritis: integrating network pharmacology and in vivo pharmacological evaluation. *Front Pharmacol*. 2017;8(MAY). doi:10.3389/fphar.2017.00230
15. Yu G, Wang W, Wang X, et al. Network pharmacology-based strategy to investigate pharmacological mechanisms of Zuojinwan for treatment of gastritis. *BMC Complement Altern Med*. 2018;18(1). doi:10.1186/s12906-018-2356-9
16. Han K, Zhang L, Wang M, Zhang R, Wang C, Zhang C. Prediction methods of herbal compounds in Chinese medicinal herbs. *Molecules*. 2018;23(9):2303. doi:10.3390/molecules23092303
17. Yu L, Wei F, Liang J, et al. Target molecular-based neuroactivity screening and analysis of panax ginseng by affinity ultrafiltration, UPLC-QTOF-MS and molecular docking. *Am J Chin Med*. 2019;47(6):1345–1363. doi:10.1142/S0192415X19500691

18. Yadav BS, Tripathi V. Recent advances in the system biology-based target identification and drug discovery. *Curr Top Med Chem*. 2019;18(20):1737–1744. doi:10.2174/1568026618666181025112344
19. Zhu Y, Zhong W, Peng J, Wu H, Du S. Study on the mechanism of baimai ointment in the treatment of osteoarthritis based on network pharmacology and molecular docking with experimental verification. *Front Genet*. 2021;12. doi:10.3389/fgene.2021.750681
20. Zhang JZ, Chen XY, Wu YJ, et al. Identification of active compounds from Yi Nationality herbal formula wosi influencing COX-2 and VCAM-1 Signaling. *Front Pharmacol*. 2020:11. doi:10.3389/fphar.2020.568585
21. Fattori V, Staurengo-Ferrari L, Zaninelli TH, et al. IL-33 enhances macrophage release of IL-1β and promotes pain and inflammation in gouty arthritis. *Inflamm Res*. 2020;69(12):1271–1282. doi:10.1007/s00011-020-01399-x
22. Vanheule V, Janssens R, Boff D, et al. The positively charged COOH-terminal Glycosaminoglycan-binding CXCL9(74-103) peptide inhibits CXCL8-induced neutrophil extravasation and monosodium urate crystal-induced gout in mice. *J Biol Chem*. 2015;290(35):21292–21304. doi:10.1074/jbc.M115.649855
23. Liu S, Yin C, Chu N, Han L, Li C. IL-8 −251T/A and IL-12B 1188A/C polymorphisms are associated with gout in a Chinese male population. *Scand J Rheumatol*. 2013;42(2):150–158. doi:10.3109/03009742.2012.726372
24. Bai B, Liu Y, Abudukerimu A, et al. Key genes associated with pyroptosis in gout and construction of a miRNA-mRNA regulatory network. *Cells*. 2022;11(20):3269. doi:10.3390/cells11203269
25. Martinon F, Pétrilli V, Mayor A, Tardivel A, Tschopp J. Gout-associated uric acid crystals activate the NALP3 inflammasome. *Nature*. 2006;440(7081):237–241. doi:10.1038/nature04516
26. Chang WC, Chu MT, Hsu CY, et al. Rhein, an anthraquinone drug, suppresses the NLRP3 inflammasome and macrophage activation in urate crystal-induced gouty inflammation. *Am J Chin Med*. 2019;47(1):135–151. doi:10.1142/S0192415X19500071
27. Clarke J. β-carotene blocks the inflammasome. *Nat Rev Rheumatol*. 2020;16(5):248. doi:10.1038/s41584-020-0415-3
28. Yan J, Zhang G, Hu Y, Ma Y. Effect of luteolin on xanthine oxidase: inhibition kinetics and interaction mechanism merging with docking simulation. *Food Chem*. 2013;141(4):2766–2773. doi:10.1016/j.foodchem.2013.06.092
29. Shi DH, Huang W, Li C, Liu YW, Wang SF. Design, synthesis and molecular modeling of aloe-emodin derivatives as potent xanthine oxidase inhibitors. *Eur J Med Chem*. 2014;75:289–296. doi:10.1016/j.ejmech.2014.01.058
30. Ruiming S, Ma L, Zheng Y, et al. Anti-inflammatory effects of luteolin on acute gouty arthritis rats via TLR/MyD88/NF-κB pathway. *J Centr South Univ Med Sci*. 2020;45(2):115–122. doi:10.11817/j.issn.1672-7347.2020.190566
31. Lin Y, Liu PG, Liang WQ, et al. Luteolin-4′-O-glucoside and its aglycone, two major flavones of Gnaphalium affine D. Don, resist hyperuricemia and acute gouty arthritis activity in animal models. *Phytomedicine*. 2018;41:54–61. doi:10.1016/j.phymed.2018.02.002
32. Wilms LC, Hollman PCH, Boots AW, Kleinjans JCS. Protection by quercetin and quercetin-rich fruit juice against induction of oxidative DNA damage and formation of BPDE-DNA adducts in human lymphocytes. *Mutat Res Genet Toxicol Environ Mutagen*. 2005;582(1–2):155–162. doi:10.1016/j.mrgentox.2005.01.006
33. Liu Y, Duan C, Chen H, et al. Inhibition of COX-2/mPGES-1 and 5-LOX in macrophages by leonurine ameliorates monosodium urate crystal-induced inflammation. *Toxicol Appl Pharmacol*. 2018;351:1–11. doi:10.1016/j.taap.2018.05.010
34. Gu H, Yu H, Qin L, et al. MSU crystal deposition contributes to inflammation and immune responses in gout remission. *Cell Rep*. 2023;42(10):113139. doi:10.1016/j.celrep.2023.113139
35. Khanna PP, Gladue HS, Singh MK, et al. Treatment of acute gout: a systematic review. *Semin Arthritis Rheum*. 2014;44(1):31–38. doi:10.1016/j.semarthrit.2014.02.003
36. Chen CJ, Shi Y, Hearn A, et al. MyD88-dependent IL-1 receptor signaling is essential for gouty inflammation stimulated by monosodium urate crystals. *J Clin Invest*. 2006;116(8):2262–2271. doi:10.1172/JCI28075
37. Schlesinger N, Thiele RG. The pathogenesis of bone erosions in gouty arthritis. *Ann Rheum Dis*. 2010;69(11):1907–1912. doi:10.1136/ard.2010.128454
38. Kienhorst L, Janssens H, Radstake T, et al. A pilot study of CXCL8 levels in crystal proven gout patients during allopurinol treatment and their association with cardiovascular disease. *Joint Bone Spine*. 2017;84(6):709–713. doi:10.1016/j.jbspin.2016.10.013
39. Köttgen A, Albrecht E, Teumer A, et al. Genome-wide association analyses identify 18 new loci associated with serum urate concentrations. *Nat Genet*. 2013;45(2):145–154. doi:10.1038/ng.2500
40. Jaramillo M, Godbout M, Naccache PH, Olivier M. Signaling events involved in macrophage chemokine expression in response to monosodium urate crystals. *J Biol Chem*. 2004;279(50):52797–52805. doi:10.1074/jbc.M403823200
41. Qing YF, Zhou JG, Zhang QB, et al. Association of TLR4 Gene rs2149356 Polymorphism with Primary Gouty Arthritis in a Case-Control Study. *PLoS One*. 2013;8(5):e64845. doi:10.1371/journal.pone.0064845
42. Terkeltaub R, Liu-Bryan R, Pritzker K, Firestein GS. Oxide generation monosodium urate crystal-induced nitric calcium pyrophosphate dihydrate and TLR2 signaling in chondrocytes drives; 2013. Available from: http://www.jimmunol.org/content/174/8/5016.full#ref-list-1. Accessed November 14, 2023.
43. Liu-Bryan R, Scott P, Sydlaske A, Rose DM, Terkeltaub R. Innate immunity conferred by Toll-like receptors 2 and 4 and myeloid differentiation factor 88 expression is pivotal to monosodium urate monohydrate crystal-induced inflammation. *Arthritis Rheum*. 2005;52(9):2936–2946. doi:10.1002/art.21238